TrajNet: An Efficient and Effective Neural Network for Vehicle Trajectory Classification

Jiyong Oh, Kil-Taek Lim and Yun-Su Chung
Daegu-Gyeongbuk Research Center, Electronics and Telecommunications Research Institute (ETRI), Daegu, Korea
{*jiyongoh, ktl, yoonsu*}*@etri.re.kr*

Keywords: Vehicle Trajectory Classification, TrajNet, Deep Neural Network, Intelligent Transportation System.

Abstract: Vehicle trajectory classification plays an important role in intelligent transportation systems because it can be utilized in traffic flow estimation at an intersection and anomaly detection such as traffic accidents and violations of traffic regulations. In this paper, we propose a new neural network architecture for vehicle trajectory classification by modifying the PointNet architecture, which was proposed for point cloud classification and semantic segmentation. The modifications are derived based on analyzing the differences between the properties of vehicle trajectory and point cloud. We call the modified network TrajNet. It is demonstrated from experiments using three public datasets that TrajNet can classify vehicle trajectories faster and more slightly accurate than the conventional networks used in the previous studies.

1 INTRODUCTION

Smart city is one of the important convergence technologies that need to be developed to improve the quality of human life. Intelligent transportation system (ITS) is a representative technology required in smart city, which makes it possible for people to use road traffic networks safely and efficiently through real-time monitoring and effective traffic control. Since vehicle trajectory has essential information about movement direction and speed of vehicles, it can be used in traffic flow estimation (Lv et al., 2015) and traffic anomaly detection (Zhao et al., 2019), which are typical applications of ITS. In this study, we focus on classifying those vehicle trajectories extracted by tracking vehicles as in (Ren et al., 2018).

Trajectory classification or clustering has been studied in various applications such as behavior analysis (Wang et al., 2008), group detection (Li et al., 2017), semantic region analysis (Wang et al., 2011), and traffic vedio surveillence (Morris and Trivedi, 2009), (Hu et al., 2013), (Lin et al., 2017). In early studies, researchers were mainly interested in the mathematical representation of trajectories and the similarity measure between them. In (Porikli, 2004), the authors proposed a new similarity measure based on the hidden Markov model, and in (Morris and Trivedi, 2009), six similarity measures were compared and evaluated for trajectory clustering. Also, in (Hu et al., 2013), the Dirichlet process mixture model (DPMM) was employed for trajectory analysis such as clustering, modeling, and retrieval. An incremental method using DPMM was developed to automatically determine the number of clusters, and a time-sensitive DPMM was also proposed to encode the time-dependent characteristics of trajectories. In (Xu et al., 2015), an effective and robust trajectory clustering method was proposed based on shrinking trajectories. The method consists of an adaptive multi-kernel estimation process and an optimization process. The adaptive multi-kernel estimation process was employed to reduce intra-variation and enlarge inter-variation between trajectories. And, the optimization process with speed regularization was introduced to utilize the shape information of the original trajectory and the discriminative information obtained from the estimation based on the adaptive multi-kernels. Moreover, in (Lin et al., 2017), the authros presented a novel representation based on a three-dimensional tube and a droplet process. Given a set of trajectories, a thermal transfer field was constructed to capture global information of the trajectories, and a three-dimensional tube was generated from each trajectory using the relation between its points and the thermal transfer field. Then, the droplet-based process was applied to provide a low dimensional droplet vector that encodes the high dimensional information in the three-dimensional tube.

After the impressive successes of deep neural networks such as (Krizhevsky et al., 2012) and (Ren

Oh, J., Lim, K-T. and Chung, Y-S.
TrajNet: An Efficient and Effective Neural Network for Vehicle Trajectory Classification.
In *Proceedings of the 10th International Conference on Pattern Recognition Applications and Methods (ICPRAM 2021)*, pages 414-422
ISBN: 978-989-758-486-2 ISSN: 2184-4313

et al., 2015), deep learning-based approaches have been applied in many studies of various applications such as human activity recognition (Yang et al., 2015) and GPS trajectory analysis (Jiang et al., 2017), (Yao et al., 2017), (Song et al., 2018). In (Yang et al., 2015), by applying a sliding window, time-series signals captured by multiple sensors split into a set of short intervals of multiple signals. The short intervals were represented as two-dimensional matrices corresponding to the input of a convolutional neural network (CNN) to solve human activity recognition problems. In (Jiang et al., 2017), a new method, TrajectoryNet, was proposed to detect human transportation mode using GPS trajectory. The proposed method extracted the segment-based features and the point-based features from GPS data. Then, the features of different types were combined and classified using an RNN based on the bidirectional maxout gated recurrent units (GRUs). In (Yao et al., 2017), a deep learning-based representation of trajectory was presented. In the study, a feature sequence was generated from a trajectory using a sliding window technique, and it was transformed into a deep representation with a fixed-size by a sequence-to-sequence autoencoder. The representation was applied in clustering and analyzing GPS trajectories. In (Song et al., 2018), taxi fraud detection was addressed using GPS trajectories. The long short term memory (LSTM) and GRU cells were utilized in RNN to solve the problem.

On the other hand, deep neural networks were also applied in traffic video surveillance (Ma et al., 2018), (Santhosh et al., 2018). In (Ma et al., 2018), trajectory distance metrics were presented to measure similarities and detect anomalous trajectories, and an RNN-based autoencoder was used in computing the metrics. Also, two different deep neural networks were used in (Santhosh et al., 2018). In the method, a CNN classifies an input trajectory converted into an image using the gradient conversion method, and a variational autoencoder decides whether the input trajectory image is an anomaly or not.

In this paper, we propose a deep neural network architecture to address the vehicle trajectory classification. Inspired from PointNet (Qi et al., 2017) that is a novel neural network proposed for classification or semantic segmentation of point cloud data, the proposed architecture is derived based on analyzing the differences between the characteristics of point cloud and trajectory. We call the new architecture *TrajNet*. To our best knowledge, this is the first study using the other network for vehicle trajectory classification instead of the conventional neural networks such as RNN, LSTM, and CNN. We demonstrate by performing experiments that the proposed method yields slightly better classification performances compared to the conventional architectures like a vanilla RNN and an RNN with LSTM unit as well as the CNN with the gradient conversion method proposed for vehicle trajectory classification in (Santhosh et al., 2018). Furthermore, it is also shown that the proposed network can classify a trajectory faster than those networks.

This paper is organized as follows. In the next section, a preprocessing method is explained together with the conventional networks which have been previously presented for the vehicle or GPS trajectory classification. The proposed network architecture is described in Sec. 3. Then, we verify in Sec. 4 that the proposed network is more effective and efficient than the other networks employed in the previous studies for the trajectory classification. Finally, we conclude this paper in the last section.

2 PRELIMINARIES

2.1 Preprocessing

One of the difficulties in using a trajectory as an input of neural networks is the fact that the number of points included in it is not the same. To input an arbitrary trajectory to a neural network, which has a regular input structure, we generate the input trajectory with M points using the cubic B-spline curves approximation as in (Ma et al., 2018). Figure 1 shows an original trajectory and the trajectories generated by the method when $M = 16$, $M = 32$, and $M = 64$. In the figure, each point in trajectories is represented as a marker located at its coordinates on the image. The color of the points is determined by the gradient conversion (Santhosh et al., 2018), in which the hue value h of the i-th point $\mathbf{p}_i$ in a trajectory $T = \{\mathbf{p}_i = (x_i, y_i)\}_{i=1}^{M}$[1] is computed as

$$h(\mathbf{p}_i) = \frac{i}{M} \times 180.$$

The other two values of the HSV color model are set to 255. We can see from the figure that each trajectory can be normalized to have a fixed number of points by the cubic B-spline curves approximation method.

[1] Each point in a trajectory can have its time step as $\mathbf{p}_i = (x_i, y_i, t_i)$, but we do not consider those time steps in this study.

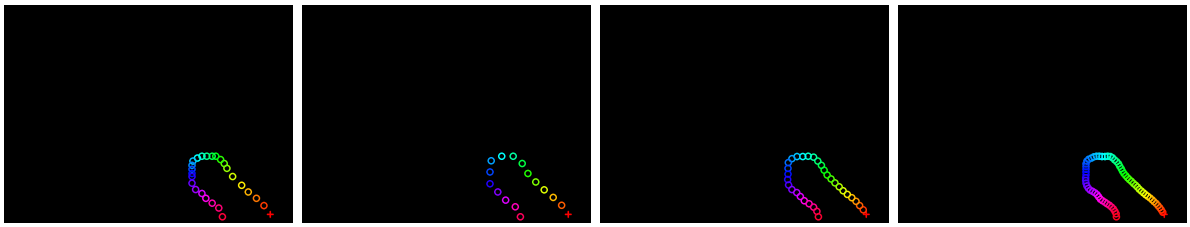

(a) Original (b) $M = 16$ (c) $M = 32$ (d) $M = 64$

Figure 1: An original trajectory with $M = 26$ and the trajectories generated by the normalization based on the cubic B-spline curves approximation. Best viewed in color.

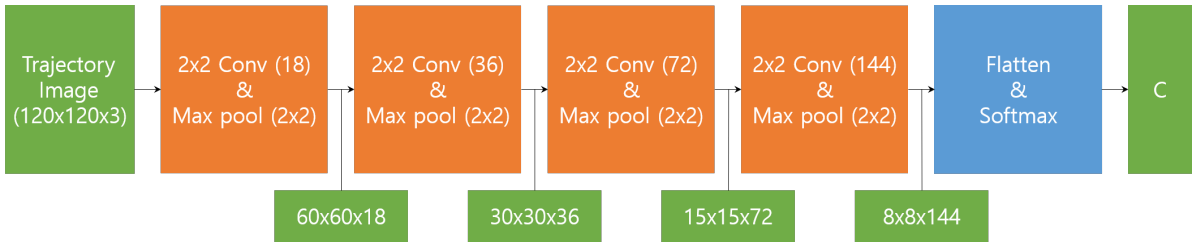

Figure 2: The architecture of CNN used in this study.

2.2 RNN and LSTM

RNN is a kind of neural network suitable for processing sequential data (Goodfellow et al., 2016). Since a vehicle trajectory is a sequence of ordered points, it is straightforward to apply an RNN to the vehicle trajectory classification. For this reason, we first consider a stacked RNN, and the number of the stacked RNN layers is set to 3 based on experiments. In each layer of the stacked RNN, the hyperbolic tangent activation function is employed in its 128-dimensional hidden state. The stacked RNN is connected to an additional fully-connected layer with the sigmoid activation function, and the dimension of the hidden layer in the fully-connected layer is also set to 128. Finally, the softmax layer follows the fully-connected layer for C-class classification. After the normalization described in the previous subsection, each point in a trajectory is input to the stacked RNN at a time, and for the trajectory, the stacked RNN provides the C-dimensional vector, each component of which corresponds to the probabilities belonging to each class.

However, it is well known that the conventional RNN has the vanishing gradient problem, which deteriorates its learning capability when the length of sequence data is longer. In order to alleviate the problem, the LSTM cell has been popularly used instead of the original RNN cell in practice. Thus, we also consider another RNN using the LSTM cells as in (Song et al., 2018) together with the conventional RNN. The LSTM-based RNN has the same architecture as the stacked RNN mentioned above except for using the LSTM cell. The two RNNs mentioned in this subsection will be applied in the vehicle trajectory classification and compared to the different types of neural networks mentioned later in Sec. 4.

2.3 CNN

CNN was originally developed to classify image data with a type of grid. Since its remarkable successes in image classification (Krizhevsky et al., 2012), it has become very popular in various fields. However, to classify a trajectory using a CNN, it should have a regular form with a pre-determined size such as an image. We convert each trajectory into an image shown in Fig. 1. Then, the generated image is input to the CNN proposed in (Santhosh et al., 2018). In the image generation, we employ the gradient conversion mentioned above because it was reported in (Santhosh et al., 2018) that the conversion method provided an additional performance increase.

Figure 2 shows the architecture of the CNN used in this study. The input trajectory image passes through the four pairs of the convolution and the max-pooling layers successively. Those convolution layers have 18, 36, 72, and 144 filters with the size of 2×2, and all of the max-pooling layers have the size of 2×2. The ReLU activation function (Nair and Hinton, 2010) is applied in all of the convolution layers. By those convolution and max-pooling layers, each trajectory image becomes a three-dimensional tensor, which is flattened as a one-dimensional vector to input to the final softmax layer for classification. For more information, refer to (Santhosh et al., 2018). Although the normalization using the gradient conver-

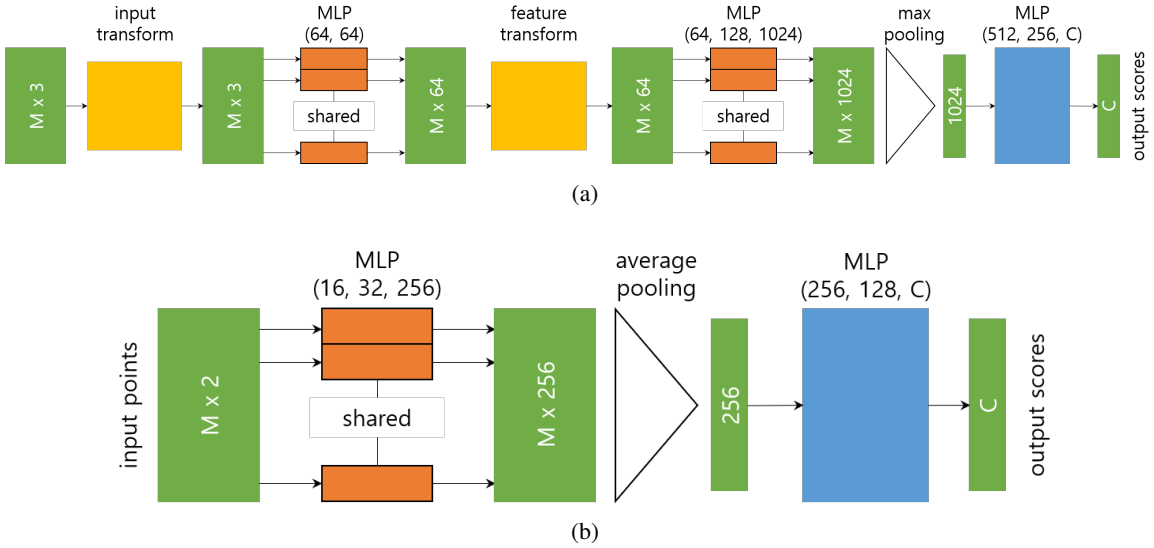

Figure 3: The archtiectures of PointNet and TrajNet. (a) PointNet for point cloud classification. (b) TrajNet using average-pooling layer (TrajNet-A) for vehicle trajectory classification. Best viewed in color.

sion and the CNN architecture seem to be simple, it was verified in (Santhosh et al., 2018) that it provided better classification performances than other methods presented for the same purpose.

3 PROPOSED METHOD

According to (Qi et al., 2017), the PointNet architecture consists of three key modules for point cloud classification and semantic segmentation. Two modules among them are related to point cloud classification, which is similar to the trajectory classification addressed in this work. Associated with the two modules, we pay attention to the differences between the properties of trajectory and point cloud. One of the differences is the fact that the points in a trajectory are ordered in time sequence different from the points in a point cloud. The next difference is related to the fact that the point cloud classification should be invariant under any rigid transformation, but we do not have to consider those transformations when classifying a trajectory in this study. Based on the above two differences, we derive a new network by modifying the architecture of PointNet. Because of the first difference, we consider using the average-pooling layer and the flatten layer along with the max-pooling layer. Note the fact that only the max-pooling layer is used in the PointNet architecture as shown in Fig. 3a. Also, PointNet has the joint alignment networks for the invariance under rigid transformations, which correspond to the blocks denoted as input transform and feature transform in Fig. 3a. However, the alignment network is not used in our architecture based on the second difference.

Based on the two modifications, we propose the TrajNet architecture as shown in Fig. 3b. It consists of three parts, the shared multi-layer perceptrons layers (MLP), the pooling layers, and the conventional MLP layers. In the figure, the average-pooling layer is used, but it can be replaced by the max-pooling layer or the flatten layer so that the proposed architecture is named as *TrajNet-M*, *TrajNet-A*, or *TrajNet-F* when using the max-pooling, the average pooling, or the flatten layer, respectively. In detail, the size of each filter in the shared MLPs is set to 1, and the numbers of those filters are determined as 16, 32, and 256. And, we set the dimensions of the two hidden layers in the conventional MLP to 256 and 128. Each layer of the shared MLPs and the conventional MLPs employ the ReLU activation function. The batch normalization (Ioffe and Szegedy, 2015) also follows each layer of the shared and conventional MLPs. Furthermore, the dropout layer (Srivastava et al., 2014) is adopted in the two conventional MLPs, and its drop rate is set to 0.7. Finally, the last layer is the softmax for classification. The above values of the parameters were determined from many trials of experiments. Note that the proposed network has a simple architecture compared to PointNet and the numbers of the neurons in the MLPs of TrajNet are reduced to a quarter or a half as shown in Fig 2. It may seem that the proposed architecture is obtained by only slight modifications of the PointNet architecture. However, it is noticeable that those modifications are based on analyzing the differences between trajectory and point

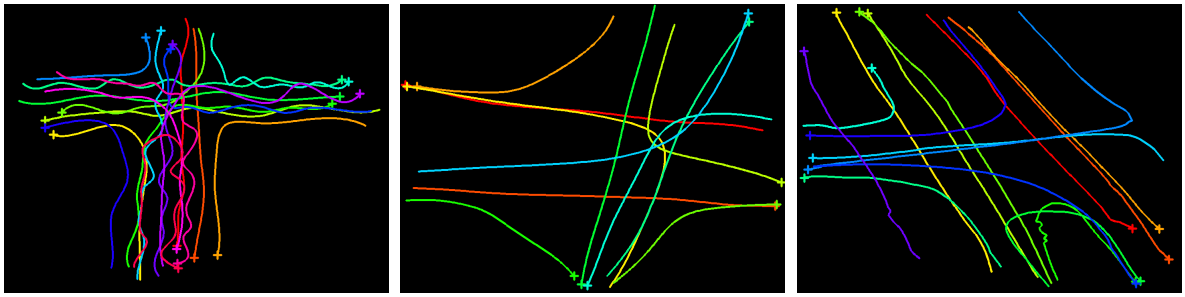

(a) CROSS dataset (b) TRAFFIC dataset (c) VMT dataset

Figure 4: Trajectory examples for three datasets. In the figures, each cross means the starting point of the trajectory. Best viewed in color.

Table 1: Datasets used in experiments.

Dataset	C	N_r	N_t	M_{min}	M_{max}
CROSS	19	1900	9500	4	30
TRAFFIC	11	300		50	50
VMT	15	1500		16	612

cloud. It will also be verified in the next section that the proposed network derived by the simple modifications is more effective and efficient than the other networks used in the previous studies for vehicle trajectory classification.

4 EXPERIMENTS

We conducted experiments using three datasets[2] to evaluate the neural networks described in the previous sections. Table 1 summarizes the three datasets and Fig. 4 shows the examples of trajectories belonging to each class in each dataset. In the table, C, N_r and N_t denote the number of classes, the number of training trajectories, and the number of test trajectories, respectively. Also, M_{min} and M_{max} denote the minimum and maximum numbers of points included in a trajectory in each dataset, respectivley. In Fig. 4, each trajectory is represented as a curve for better visualization, but it consists of two-dimensional points in actual. Among the datasets, the CROSS dataset (Morris and Trivedi, 2009) has the trajectories generated by simulating vehicle movements at a four-way intersection. This dataset provides a training set and a test set separately. Each trajectory belongs to one of 19 classes, but its test set contains the trajectories that do not belong to any class in the training set. Although they can be used for anomaly detection as in (Ma et al., 2018) and (Santhosh et al., 2018), they were not used in this study to focus on the trajectory classification. On the other hand, different from the CROSS dataset, the TRAFFIC (Lin et al., 2017) and VMT (Morris and Trivedi, 2011) datasets consist of the real trajectories extracted by tracking vehicles captured by a mounted intersection monitoring camera. The TRAFFIC and VMT datasets consist of 11 and 15 classes, respectively, as in Table 1.

Another difference between the CROSS dataset and the other datasets is the fact that the TRAFFIC and VMT datasets are not divided as the training set and test set. In this situation, one of the most general evaluation methodologies is cross validation. We also performed the two- and five-fold cross validations using the TRAFFIC and VMT datasets, respectively, to evaluate the performance of the proposed networks. In K-fold cross validation, the whole trajectories in a dataset were divided into K folds. The performance of each network is evaluated using the trajectories in a fold after training the network using the trajectories in the other $K-1$ folds. These training and testing procedures are repeated K times utilizing each fold for testing and the other folds for training at a time.

We first compared the neural networks mentioned in the previous sections in terms of classification accuracy. The classification accuracy of a network was computed as

$$\frac{N_c}{N} \times 100,$$

where N_c is the number of the trajectories that are correctly classified among the test trajectories and N is the number of the whole test trajectories. However, due to the randomness in weight initialization, the value of N_c may vary even if the same learning is repeated. To avoid the problem, we computed the classification accuracy whenever the weights of a network are updated using a mini-batch, and then repeated the same training and evaluation ten times for a given pair of the training and test sets. We selected the maximum value of N_c to compute the classification accu-

[2]The datasets were downloaded from https://github.com/mcximing/ACCV18_Anomaly/tree/master/Exp2/datasets

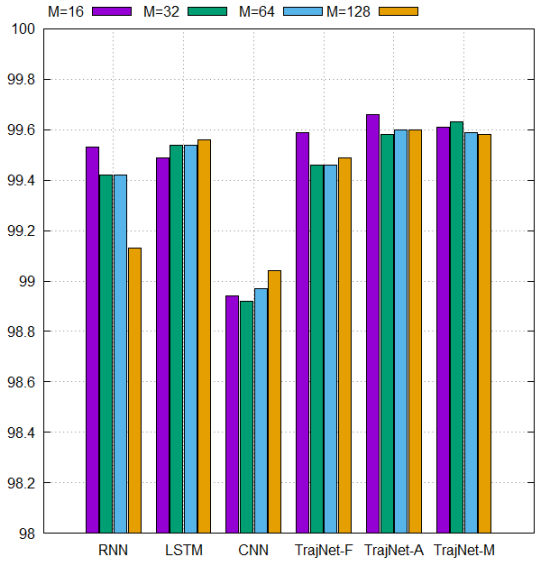

Figure 5: Classification results for CROSS dataset. Best viewed in color.

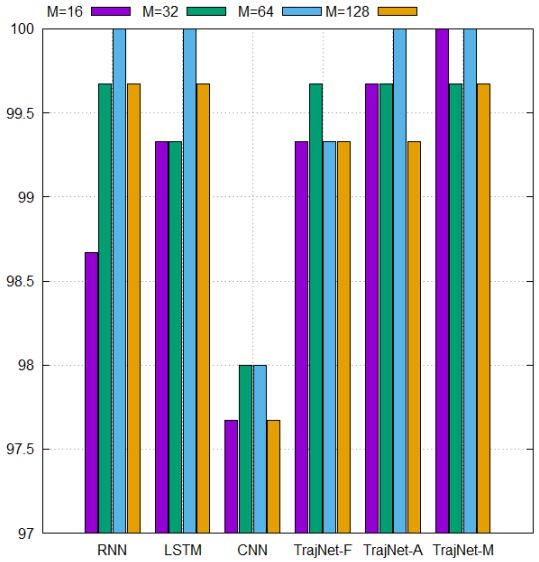

Figure 6: Classification results for TRAFFIC dataset. Best viewed in color.

racy in those repetitive training and testing. In the K-cross validation, the maximum number of the correctly classified trajectories was selected for each pair of training and test sets, and the value of N_c was determined by adding the K maximum numbers for all of the pairs of the training and test sets.

We implemented all of the methods described in this section using TensorFlow (Abadi et al., 2015). The cross entropy was chosen as the loss function in training all of the networks, and we adopted the Adam optimizer (Kingma and Ba, 2015) with the learning rate of 0.001 to minimize (maximize) the loss function. The size of the mini-batch was set to 100 when training all of the networks. From many trials of those network training, the maximum number of epochs was set to 500, 500, 50, and 400 for RNN, LSTM, CNN, and TrajNets, respectively. This means that CNN could be easily trained compared to the other networks. To examine the relationship between the number of points in trajectories and the classification performance, we performed the experiments by varying the value of M as 16, 32, 64, and 128.

Figures 5, 6, and 7 show the classification accuracies for the CROSS, TRAFFIC, VMT datasets, respectively. It is shown in Fig. 5 that all of the networks provided classification accuracies over 99% on average except for CNN, which showed its average accuracy of 98.97% for the CROSS dataset. In particular, TrajNet-A and TrajNet-M, which are the proposed networks, yielded the best average performances over 99.6%, and TrajNet-A obtained the highest classification accuracy with $M = 16$. We can see that RNN yielded lower classification accuracies as M increases. This agrees with the fact well-known in the literature that the learning capability of RNN decreases when the length of the sequence data increases. However, the proposed networks can provide slightly higher accuracies with the small numbers of M than RNN, LSTM, and CNN. Since the time required for the inference of an arbitrary trajectory increases with the value of M, this means that the proposed network can classify trajectories in a shorter time. Figure 6 shows the classification accuracies of the networks on the TRAFFIC dataset. Similar to the CROSS dataset, we can see that CNN provided the lowest classification accuracies for all the values of M. Note that the 100% classification accuracy was obtained by RNN, LSTM, TrajNet-A, and TrajNet-M when $M = 64$. However, TrajNet-A and TrajNet-M yielded the highest average accuracies of 99.67% and 99.84%, respectively, and TrajNet-M provided 100% accuracy when $M = 16$ as well as $M = 64$. Figure 7 shows the classification accuracies on the VMT dataset. We can see again that the accuracy of RNN decreases relatively large as the value of M increases. On average, TrajNet-A, TrajNet-M, and LSTM provided the highest accuracies of 99.10%, 99.02%, and 99.00%, respectively. It is notable that TrajNet-A provided the best accuracies for $M = 16$, $M = 32$, and $M = 128$. In particular, the highest accuracy of 99.2% on this dataset was obtained by TrajNet-A when $M = 16$. In total, it may seem that the accuracy improvement of the proposed networks is marginal. However, the improvements are not meaningless because RNN, LSTM, and CNN already give very high accuracies of around 99%.

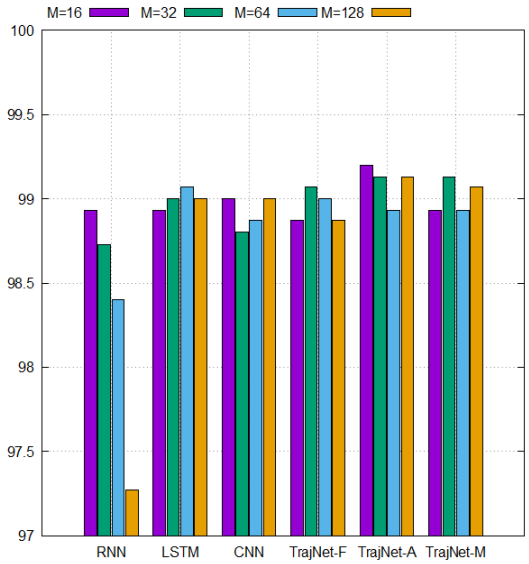

Figure 7: Classification results for VMT dataset. Best viewed in color.

Together with the classification accuracy, the classification speed and the number of parameters are also important performance of classification methods. We measured the inference time required to classify trajectories and counted the number of parameters in the networks. Table 2 shows the time to classify the 9500 test trajectories in the CROSS dataset after training each network for all the values of M. It was measured on a PC with a GPU of TITAN Xp. In the case of CNN, the time required in the conversion from an input trajectory to an image was not included in the inference time. The table shows that the proposed networks can classify input trajectories faster than RNN, LSTM, and CNN for each value of M. In particular, when $M = 16$, TrajNet-A, which gave better classification accuracies, required about 40%, 59%, and 45% of the inference times of RNN, LSTM, and CNN, respectively. Note that those speed improvements were achieved together with the improvement in the classification accuracy, not its sacrifice. As M increases, we can see that the inference time increases in all of the networks except CNN. However, the ones of TrajNets increase slower than the ones of RNN and LSTM. It can be expected from this result that the trajectory classification based on TrajNet can be performed much faster than RNN or LSTM in a situation that the points included in trajectories become more and more. Interestingly, TrajNet-F showed the fastest inference time even though it contains the maximum number of parameters for the same value of M. We expect from this result that the architecture of TrajNet-F is more appropriate to the use of GPU than the other architectures. Another superiority of the proposed networks can be seen in Table 3, which summarizes the number of parameters for each value of M. We can see from the table that regardless of the value of M, the numbers of parameters included in all of the networks remain the same except TrajNet-F. Among those networks, the two proposed networks, TrajNet-A and TrajNet-M, contain the lowest numbers of parameters except for RNN.

Table 2: Inference time required to classify 9500 test trajectories in CROSS dataset (in seconds).

Network	$M = 16$	$M = 32$	$M = 64$	$M = 128$
RNN	2.142	3.687	7.661	15.941
LSTM	1.466	1.713	2.126	2.855
CNN	1.926	1.919	1.923	1.921
TrajNet-F	0.549	0.600	0.615	0.714
TrajNet-A	0.865	0.882	0.971	1.097
TrajNet-M	0.930	0.954	1.017	1.143

Table 3: Number of parameters in network (in thousands).

Network	$M = 16$	$M = 32$	$M = 64$	$M = 128$
RNN	102	102	102	102
LSTM	351	351	351	351
CNN	189	189	189	189
TrajNet-F	1095	2145	4241	8436
TrajNet-A	113	113	113	113
TrajNet-M	113	113	113	113

In summary, it was demonstrated from our experimental results on the three datasets that TrajNet can classify an input trajectory faster and more accurately than the other deep networks presented in the previous studies, and the proposed architecture with the average-pooling or the max-pooling layer can also be stored in a less memory space than LSTM and CNN.

5 CONCLUSIONS

In this paper, we proposed a new network architecture to address the vehicle trajectory classification. Inspired from PointNet (Qi et al., 2017), which has a novel architecture to deal with point cloud classification and semantic segmentation, the proposed architecture was derived based on analyzing the difference between the properties of the trajectory and the point cloud. From our experiments using the three public datasets, we show that the proposed architecture could provide slight improvements in the classification accuracy over RNN, LSTM, and CNN, which yielded

sufficiently high classification accuracies. Furthermore, it was verified that TrajNet-A, one of the proposed networks, could classify the test trajectories of the CROSS dataset in 40%, 59%, and 45% less time than RNN, LSTM, and CNN, respectively, under the setting of $M = 16$ along with the accuracy improvements. In terms of memory space, TrajNet-A and TrajNet-M require lower numbers of parameters than LSTM and CNN. Also, we could see from the experiments that the number of points included in a trajectory has little effect on the classification accuracy except for RNN.

In future work, the proposed networks will be applied in classifying the vehicle trajectories extracted from various real traffic situations with trajectory generation methods for traffic flow measurement and anomaly detection at intersections. Moreover, we expect that the proposed networks can be utilized in classifying trajectories obtained in other applications such as online handwriting recognition (Kim and Sin, 2014) and human activity recognition (Anguita et al., 2013).

ACKNOWLEDGEMENTS

This work was supported by Electronics and Telecommunications Research Institute (ETRI) grant funded by the Korean government [20ZD1110, Development of ICT Convergence Technology for Daegu-Gyeongbuk Regional Industry].

REFERENCES

Abadi, M., Agarwal, A., Barham, P., Brevdo, E., Chen, Z., Citro, C., Corrado, G. S., Davis, A., Dean, J., Devin, M., Ghemawat, S., Goodfellow, I., Harp, A., Irving, G., Isard, M., Jia, Y., Jozefowicz, R., Kaiser, L., Kudlur, M., Levenberg, J., Mané, D., Monga, R., Moore, S., Murray, D., Olah, C., Schuster, M., Shlens, J., Steiner, B., Sutskever, I., Talwar, K., Tucker, P., Vanhoucke, V., Vasudevan, V., Viégas, F., Vinyals, O., Warden, P., Wattenberg, M., Wicke, M., Yu, Y., and Zheng, X. (2015). TensorFlow: Large-Scale Machine Learning on Heterogeneous Systems. Software available from tensorflow.org.

Anguita, D., Ghio, A., Oneta, L., Parra Perez, X., and Reyes Ortiz, J. L. (2013). A public domain dataset for human activity recognition using smartphones. In *Proceedings of the 21th International European Symposium on Artificial Neural Networks, Computational Intelligence and Machine Learning*, pages 437–442.

Goodfellow, I., Bengio, Y., and Courville, A. (2016). *Deep Learning*. The MIT Press.

Hu, W., Li, X., Tian, G., Maybank, S., and Zhang, Z. (2013). An Incremental DPMM-Based Method for Trajectory Clustering, Modeling, and Retrieval. *IEEE Transactions on Pattern Analysis and Machine Intelligence*, 35(5):1051–1065.

Ioffe, S. and Szegedy, C. (2015). Batch Normalization: Accelerating Deep Network Training by Reducing Internal Covariate Shift. In *ICML'15: Proceedings of the 32nd International Conference on International Conference on Machine Learning*, volume 37, pages 448–456.

Jiang, X., de Souza, E. N., Pesaranghader, A., Hu, B., Silver, D. L., and Matwin, S. (2017). TrajectoryNet: An Embedded GPS Trajectory Representation for Point-based Classification Using Recurrent Neural Networks. In *Proceedings of the 27th Annual International Conference on Computer Science and Software Engineering*, pages 192–200.

Kim, J. and Sin, B.-K. (2014). Online Handwriting Recognition. In Doermann, D. and Tombre, K., editors, *Handbook of Document Image Processing and Recognition*, pages 887–915. Springer London, London.

Kingma, D. and Ba, J. (2015). Adam: A Method for Stochastic Optimization. *International Conference on Learning Representations (ICLR)*.

Krizhevsky, A., Sutskever, I., and Hinton, G. E. (2012). ImageNet Classification with Deep Convolutional Neural Networks. In *Advances in Neural Information Processing Systems 25*, pages 1097–1105.

Li, X., Chen, M., Nie, F., and Wang, Q. (2017). A Multiview-Based Parameter Free Framework for Group Detection. In *Proceedings of the Thirty-First AAAI Conference on Artificial Intelligence*, pages 4147–4153. AAAI Press.

Lin, W., Zhou, Y., Xu, H., Yan, J., Xu, M., Wu, J., and Liu, Z. (2017). A Tube-and-Droplet-Based Approach for Representing and Analyzing Motion Trajectories. *IEEE Transactions on Pattern Analysis and Machine Intelligence*, 39(8):1489–1503.

Lv, Y., Duan, Y., Kang, W., Li, Z., and Wang, F. (2015). Traffic Flow Prediction With Big Data: A Deep Learning Approach. *IEEE Transactions on Intelligent Transportation Systems*, 16(2):865–873.

Ma, C., Miao, Z., Li, M., Song, S., and Yang, M.-H. (2018). Detecting Anomalous Trajectories via Recurrent Neural Networks. In Jawahar, C., Li, H., Mori, G., and Schindler, K., editors, *Computer Vision – ACCV 2018*, pages 370–382, Cham. Springer International Publishing.

Morris, B. T. and Trivedi, M. (2009). Learning Trajectory Patterns by Clustering: Experimental Studies and Comparative Evaluation. In *2009 IEEE Conference on Computer Vision and Pattern Recognition*, pages 312–319.

Morris, B. T. and Trivedi, M. M. (2011). Trajectory Learning for Activity Understanding: Unsupervised, Multilevel, and Long-Term Adaptive Approach. *IEEE Transactions on Pattern Analysis and Machine Intelligence*, 33(11):2287–2301.

Nair, V. and Hinton, G. E. (2010). Rectified Linear Units Improve Restricted Boltzmann Machines. In *Proceedings of the 27th International Conference on Machine Learning*, pages 807–814. Omnipress.

Porikli, F. (2004). Trajectory Distance Metric Using Hidden Markov Model based Representation. In *Sixth IEEE International Workshop on Performance Evaluation of Tracking and Surveillance*.

Qi, C. R., Su, H., Mo, K., and Guibas, L. J. (2017). PointNet: Deep Learning on Point Sets for 3D Classification and Segmentation. In *2017 IEEE Conference on Computer Vision and Pattern Recognition (CVPR)*, pages 77–85.

Ren, S., He, K., Girshick, R., and Sun, J. (2015). Faster R-CNN: Towards Real-Time Object Detection with Region Proposal Networks. In *Advances in Neural Information Processing Systems 28*, pages 91–99.

Ren, X., Wang, D., Laskey, M., and Goldberg, K. (2018). Learning Traffic Behaviors by Extracting Vehicle Trajectories from Online Video Streams. In *2018 IEEE 14th International Conference on Automation Science and Engineering (CASE)*, pages 1276–1283.

Santhosh, K. K., Dogra, D. P., Roy, P. P., and Mitra, A. (2018). Video Trajectory Classification and Anomaly Detection Using Hybrid CNN-VAE. *CoRR*, abs/1812.07203.

Song, L., Wang, R., Xiao, D., Han, X., Cai, Y., and Shi, C. (2018). Anomalous Trajectory Detection Using Recurrent Neural Network. In Gan, G., Li, B., Li, X., and Wang, S., editors, *Advanced Data Mining and Applications*, pages 263–277, Cham. Springer International Publishing.

Srivastava, N., Hinton, G., Krizhevsky, A., Sutskever, I., and Salakhutdinov, R. (2014). Dropout: A Simple Way to Prevent Neural Networks from Overfitting. *Journal of Machine Learning Research*, 15:1929–1958.

Wang, J. M., Fleet, D. J., and Hertzmann, A. (2008). Gaussian Process Dynamical Models for Human Motion. *IEEE Transactions on Pattern Analysis and Machine Intelligence*, 30(2):283–298.

Wang, X., Ma, K. T., Ng, G.-W., and Grimson, W. L. (2011). Trajectory Analysis and Semantic Region Modeling Using Nonparametric Hierarchical Bayesian Models. *International Journal of Computer Vision*, 95:287–312.

Xu, H., Zhou, Y., Lin, W., and Zha, H. (2015). Unsupervised Trajectory Clustering via Adaptive Multi-kernel-Based Shrinkage. In *2015 IEEE International Conference on Computer Vision (ICCV)*, pages 4328–4336.

Yang, J. B., Nguyen, M. N., San, P. P., Li, X. L., and Krishnaswamy, S. (2015). Deep Convolutional Neural Networks on Multichannel Time Series for Human Activity Recognition. In *Proceedings of the Twenty-Fourth International Joint Conference on Artificial Intelligence (IJCAI)*, pages 3995–4001.

Yao, D., Zhang, C., Zhu, Z., Huang, J., and Bi, J. (2017). Trajectory clustering via deep representation learning. In *2017 International Joint Conference on Neural Networks (IJCNN)*, pages 3880–3887.

Zhao, J., Yi, Z., Pan, S., Zhao, Y., Zhao, Z., Su, F., and Zhuang, B. (2019). Unsupervised Traffic Anomaly Detection Using Trajectories. In *The IEEE Conference on Computer Vision and Pattern Recognition (CVPR) Workshops*.